Proc. of the 9th Intl. Conf. of Asian Society for Precision Engg. and Nanotechnology (ASPEN 2022)
15–18 November 2022, Singapore. Edited by Nai Mui Ling Sharon and A. Senthil Kumar
doi://10.3850/978-981-18-6021-8_OR-03-0163

The Influence of Laser Surface Remelting (LSR) on the Surface Morphology and in vitro Cell Viability of Additively Manufactured 316L Stainless Steel Bone Plate

Wenhe Feng[1,*], Niyou Wang[2], Yin Chi Wan[1], Paul Lim Guang Hui[1], Lina Yan[2], Gavin Kane O'Neill[3]

1 Singapore Institute of Manufacturing Technology (SIMTech), Agency for Science, Technology and Research (A*STAR) Research Entities, 2 Fusionopolis Way, #08-04 Innovis, Singapore 138634
2 Department of Mechanical Engineering, 9 Engineering Drive 1, #07-08 Block EA, National University of Singapore, Singapore 117575
3 Division of Musculoskeletal Trauma, Department of Orthopaedic Surgery, NUHS Tower Block Level 11, National University Hospital, 1E Kent Ridge Road, Singapore 119228

KEYWORDS: Laser, Surface Remelting, Additive Manufacturing, Post-process, Cytotoxicity

Additive manufacturing (AM) technologies, for instance, selective laser melting (SLM), have been used to produce orthopaedic metal implants such as bone plates to cater for the fracture fixation needs of patients. The rough and particulate surface is likely to contain loose residual metal powder soluble in vivo, thus presenting a risk of metal toxicity causing harmful effects to the nearby cells and tissue, eventually leading to revision surgery. As a post-process to improve the surface quality, laser surface remelting (LSR) can be applied to eliminate surface pores and residual powder to consequently reduce the health risks. In this study, a 100 W, 1064 µm nanosecond-pulsed laser was used to remelt the surfaces of a simulated 316L stainless steel bone plate placed in argon gas protection. A pore-free and crack-free surface layer was formed on both flat surfaces and lattice structures at a processing efficiency of 100 sec/cm^2 area. The surface asperities were removed and consequently the Sa roughness was reduced from 3.10 to 2.86 µm after LSR, but still subject to the inherited waviness. Subsequent in vitro cell viability tests presented no significant adverse effects of human osteoblast-like SAOS2 cells' viability.

1. Introduction

The advancement of AM technologies has allowed for rapid customisation of orthopaedic implants to meet clinical needs. Powder bed fusion (PBF) techniques such as SLM or e-beam melting (EBM) were commonly adopted for constructing the customised implants. However, the rough particulate surface of the as-received parts poses challenges to patient welfare because of the high likelihood of residual entrained metal powder, which is soluble and bioactive in vivo, presenting a risk of metal toxicity and hypersensitivity [1]; the porosity of the surface also increases the probability of bacterial colonisation [2]. Thus, a few types of post-processes have been adopted to improve the biocompatibility for AM implants by removing the residual powder and surface asperities, such as vibratory finishing by jostling parts around in a tub of sanding or polishing media with the limitations of finishing delicate features may not hold up well to this process; sandblasting utilising small and hard balls impacting the surface of materials with high kinetic energy, which cause elastic and plastic deformation [3] or removal of imperfections [4] to the surface but with problems of deformation of thin parts [5] as well as microcracks [6]; or chemical polishing using HF/HNO_3 solutions but requires careful handling and disposal of the material-specific acidic etchant. In contrast, laser surface remelting (LSR) flattens the surface by exploiting the surface tension of the molten material [7, 8, 9]. LSR as a post-process for AM parts presents a potential for higher productivity, better consistency and feasibility for automation. Specifically, compared to conventional surface finishing techniques, LSR offers a unique "sealing" feature to eliminate the surface pores and residual powder by remelting them into a flat and uniform remelting surface layer, and consumes no acid or grit and hence causes lower environmental impact. Hence, LSR has become a potent candidate technique for the post-processing of additively manufactured orthopaedic implants.

In this study, we investigated the effects of LSR to modify the surface properties of SLM-fabricated 316L stainless steel and the consequential effects of in vitro biocompatibility of the human osteoblast-like SAOS2 cells.

2. Material and Methods

2.1 The Bone Plate

The bone plate was additively manufactured using selective laser melting (SLM) from 316L stainless steel powder. It consisted of an octahedron lattice structure for lightweighting. The bone plate size was 120*15*6 mm. The strut diameter was 0.65 mm.

2.2 Laser Surface Remelting

The LSR utilises a high-power laser beam to remelt the surface asperities including the loose powder, embedded powder and pores of the material into a remelting layer with a reduced roughness due to the fluid infill during the process (Fig. 1 (a)). The LSR experimental setup used for this study is illustrated in Fig. 1 (b). The process was conducted using a 1064 nm wavelength, 100 W fibre laser (Rofin Powerline F 100) focused by a 160 mm f-theta lens. At a maximum repetition rate of 200 kHz, the laser pulse duration was around 100 ns. The sample surface was placed 12.5 mm off-focus to avoid excessive laser intensity causing ablation; the estimated spot size was 500 µm. A bidirectional raster scan strategy (Fig. 1 (c)) was adopted with various hatching distances. To prevent oxidation of the test plate during the LSR process, a customised, 3D-printed nylon chamber was implemented. By purging out the air using argon gas from the bottom of the chamber, a near-static Ar environment with <3 ppm oxygen enveloped the stainless steel bone plate. The laser beam was able to transmit through the UV grade fused silica glass window, which permitted a 94% transmission at the laser wavelength.

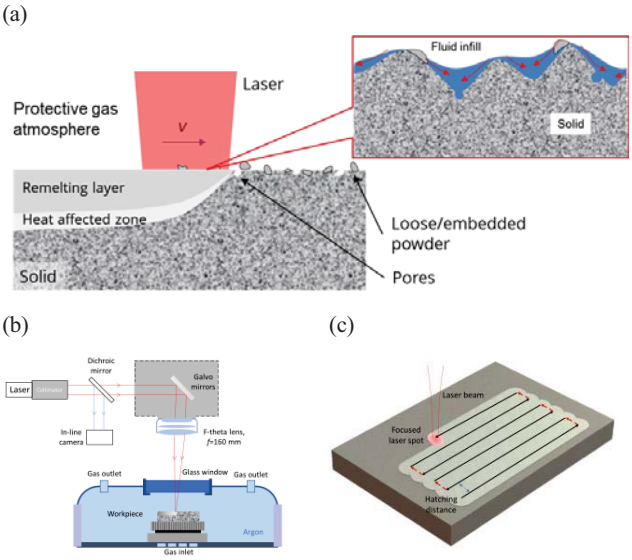

Figure 1 (a) Schematic of the LSR technique. (b) Schematic of the LSR experimental setup. (c) The bi-directional raster scan strategy.

2.3 Biocompatibility Test

An indirect cytotoxicity test was conducted on the as-received and laser surface remelted (LSR) bone plates cut to a 120*15*6 mm size to characterise the LSR's effects on the biocompatibility.

Cell culture: SAOS2 Cells (human bone osteoblastoma – HTB-85) were purchased from ATCC (American Type Culture Collection, VA, USA), and were cultured within T75 flask using McCoy's 5A media (modified, ThermoFisher Scientific, Massachusetts, USA) supplemented with 10% Heat inactivated Hyclone Fetal Bovine Serum (FBS, Utah, USA) and 1% penicillin-streptomycin (P/S, Gibco-Invitrogen, WA, USA) in a cell culture condition of 5% CO_2 and 37°C. The cells were cultured and allowed to reach 80-90% confluency. The cell culture media was changed every 1-2 days before subculture or seeding for further experiments.

Preparation of conditionalised media: as-received and LSR bone plates were immersed (total 4 types) in 70% ethanol for 2 hours and rinsed with phosphate buffer solution (PBS) 3 times thoroughly, followed by UV sterilisation for 2 hours. The plates were soaked within 10 ml complete media in 10 cm petri dish individually (complete media: McCoy's 5A media with 10% FBS and 1% P/S) for 1, 2 and 4 days before they were removed from the media. The remaining media were known as conditionalised media and named as D1M, D2M, and D4M, which were later used to culture the SAOS2 cells for following tests.

Indirect cytotoxicity test: Cell viability tests were performed using an indirect method described in previous studies [10]. SAOS2 cells were seeded into the 96-well plates at a density of 10,000 cells per well for attachment overnight in McCoy's 5a complete media. On the following day, the complete media was replaced with conditionalised media (D1M, D2M, and D4M) cultured for 5 days. Cell viabilities were determined after the particular time intervals by MTS assay using CellTiter96 Aqueous One Solution Assay (Promega, USA), according to manufacturer's protocol, and the readings were measured at 490 nm using a spectrophotometer (Tecan Infinite F200 Pro, Männedorf, Switzerland).

Statistical analysis: The data of the cell viability was analysed as the mean ± standard error of the mean (SEM) with at least 4 biological replicates (N=4). The statistical analyses were carried out using one-way ANOVA. The differences were considered statically significant with p values of $p < 0.05$, $p < 0.01$ and $p < 0.001$.

3. Results and Discussions

The appearances of the as-received and LSR samples are illustrated in Fig. 2 (a). The LSR was then applied to both flat and lattice side of the bone plate using 16 sets of laser processing parameters with various speeds (10, 20, 30 and 40 mm/s) and hatching distances (50, 100, 150 and 200 µm) as listed in Table *1*, and the processed area was 5 by 5 mm. It could be seen that LSR has improved the surface quality with the appearance being significantly more reflective compared to the as-received plate.

The SEM images of the plates are illustrated in Fig. 2 (b). Under a magnification of 40 ×, LSR significantly modified the surface morphology by transforming the rough surface to polished smooth tracks with widths close to their respective designated hatching distances. The shallow grooving along the boundary of grains was also observable with a different contrast to the polished surface. However, the laser finishing had a limitation as the laser beam could only reach those surface locations without blockage in the beam path. As shown in Fig. 2 (c), this limitation meant that only the top side of the struts were finished; the bottom side of the struts was less so as it could not

be irradiated by laser beam. None-the-less, the total surface area of exposed pores and powder was reduced.

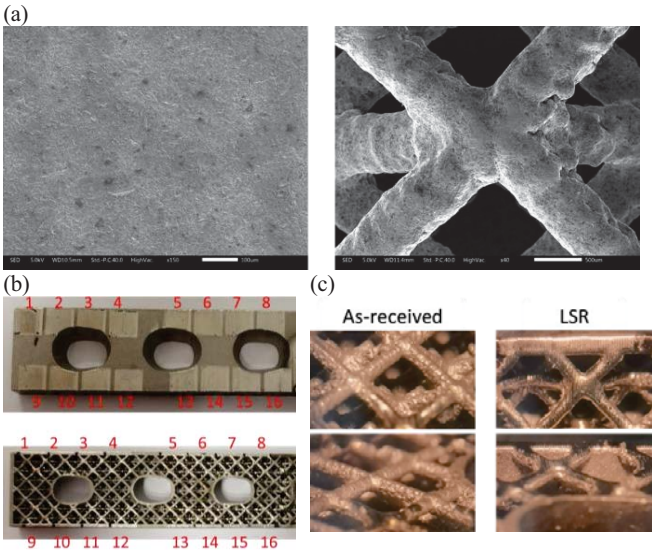

Figure 2 (a) SEM images of as-received 316L stainless steel bone plate. (b) Flat and lattice sides of the processed bone plate; 16 parameter sets were tested. (c) Microscope images of the lattice struts before and after LSR.

Table 1 The LSR Processing Parameter Sets

No.	Speed (mm/s)	Hatching distance (µm)	No.	Speed (mm/s)	Hatching distance (µm)
1	10	50	**9**	10	150
2	20	50	**10**	20	150
3	30	50	**11**	30	150
4	40	50	**12**	40	150
5	10	100	**13**	10	200
6	20	100	**14**	20	200
7	30	100	**15**	30	200
8	40	100	**16**	40	200

Via the SEM inspection, a processing window was characterised as shown in Fig. 3 demonstrated 3 typical types of results:

- The overmelt regime was characterised by the surface overmelting (SOM) which either caused surface to form drop pellets or reduction of strut thickness due to the surface tension that pulls the material toward the joints. This might reduce the total strength of the bone plate and hence should be avoided.
- The acceptable regime should also be in the SOM range, presenting reduced asperities, no visible cracks or pores and no obvious change in strut thickness, which were achievable in an optimal processing window of parameter sets.
- The undermelt regime was characterised by the surface shallow melting (SSM) where some of the original adversities were still present.

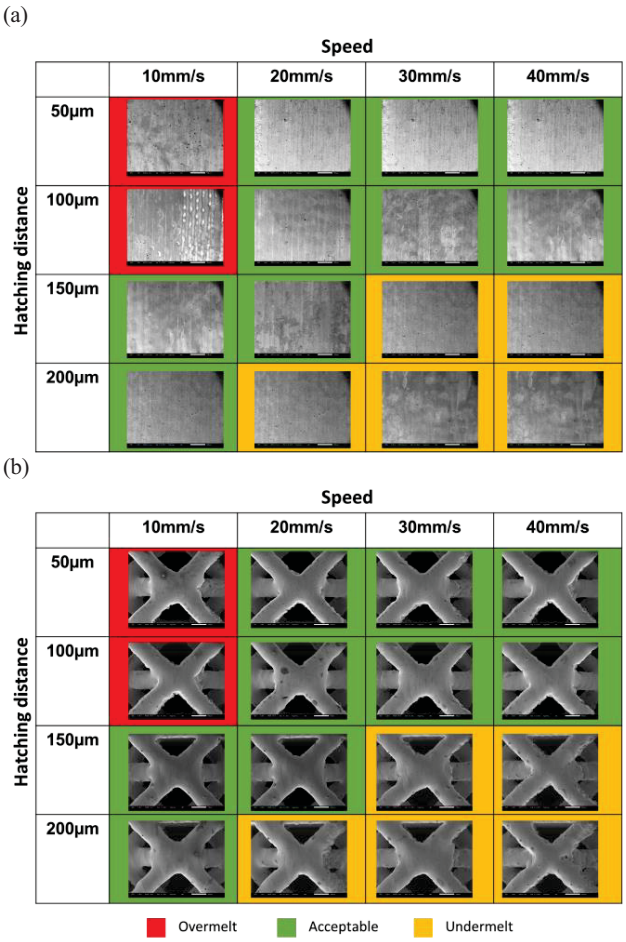

Figure 3 The parameter window for the LSR of bone plate's (a) flat and (b) lattice sides.

For the cell viability tests, two smaller bone plate samples were then cut from an as-received bone plates to a 120*15*6 mm and one of them was LSR processed using 20 mm/s, 50 µm hatching distance (parameter set no. 2) and all 6 surfaces were processed. This set provided a processing efficiency of 100 sec/cm^2. After the LSR, an optical surface profiler (Infinite Focus, Alicona) was used to obtain the optical microscopic images and to analyse the surface roughness (Sa). The results are shown in Fig. 4 (a) and it was measured that the Sa roughness was reduced from 3.10 to 2.86 µm after LSR. The in vitro indirect cytotoxicity tests on both LSR and as-received samples are shown in Fig. 4 (b). It could be seen that the cell viability of SAOS2 cells was slightly increased for both samples compared to the negative control fresh media. As for the effects of LSR, after 5 days of incubation, it can be seen that cell viability % in D4M was slightly higher compared to the as-received sample, yet slightly decreased for D1M, and D2M. In general, LSR showed no significant adverse effects compared to as-received bone plate.

(a)

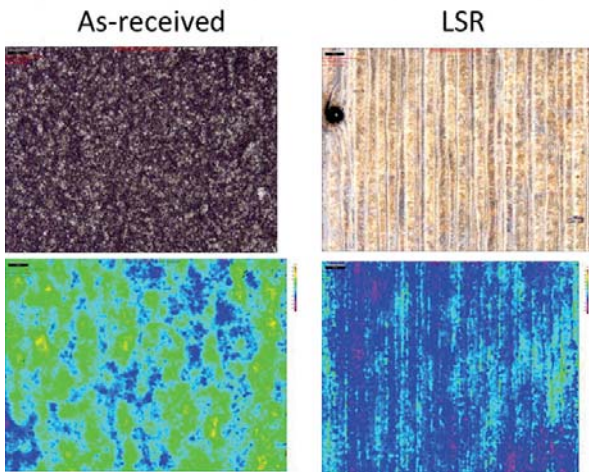

(b)

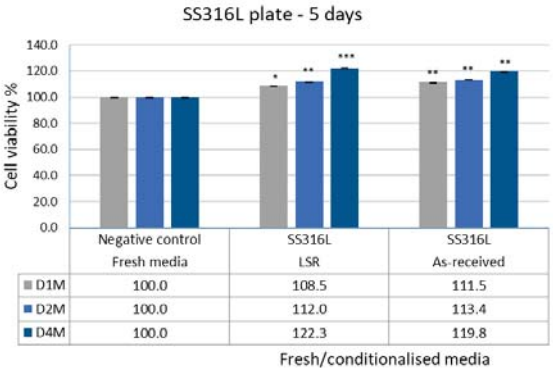

	Negative control Fresh media	SS316L LSR	SS316L As-received
D1M	100.0	108.5	111.5
D2M	100.0	112.0	113.4
D4M	100.0	122.3	119.8

*Figure 4 (a) Optical profilometer images of as-received and LSR surfaces. (b) Cell viability of SAOS2 cells cultured with conditionalised media of LSR and as-received bone plates for 5 days, respectively. N=4, Symbol * indicates a statistically significant difference, "*" indicates P < 0.05, "**" indicates P < 0.01, "***" indicates P < 0.001. Error bars denote the standard error.*

4. Conclusions

In this study, we demonstrated a laser surface remelting (LSR) technique using nanosecond-pulsed laser beam raster scanning to modify the surface of a 316L stainless steel bone plate fabricated by selective laser melting (SLM). The surface asperities were removed and consequently the Sa roughness was reduced from 3.10 to 2.86 µm after LSR, but still subject to the inherited waviness. The SEM inspection suggested that a processing window existed to achieve pore-free and crack-free remelted surface. It was observed in subsequent indirect cytotoxicity tests that human osteoblast-like SAOS2 cells' viability was not significantly affected in the conditionalised media extracted from the LSR plate compared to the as-received bone plate. In all, this study showed that the LSR introduced no adverse effects on the surface and biocompatibility properties of additively manufactured 316L stainless steel, and can potentially serve as a promising contactless post-processing tool to improve the biocompatibility of additively-manufactured orthopaedic implants in vivo.

ACKNOWLEDGEMENT

This work is supported by National Additive Manufacturing Innovation Cluster (NAMIC), Singapore. Grant No. 2019059.

References

[1] W. Z. Teo and P. C. Schalock, "Metal hypersensitivity reactions to orthopedic implants," *Dermatology and therapy ,* vol. 7, no. 1, pp. 53-64, 2017.

[2] A. Braem, L. V. Mellaert, D. Hofmans, E. D. Waelheyns, J. S. J. Anné and J. Vleugels, "Bacterial colonisation of porous titanium coatings for orthopaedic implant applications–effect of surface roughness and porosity," *Powder Metallurgy,* vol. 56, no. 4, pp. 267-271, 2013.

[3] L. Xie, J. Zhang, C. Xiong, L. Wu, C. Jiang and W. Lu, "Investigation on experiments and numerical modelling of the residual stress distribution in deformed surface layer of Ti–6Al–4V after shot peening," *Materials & Design,* vol. 41, pp. 314-318, 2012.

[4] X. Wang, Y. Fu, S. Li and H. Gao, "Finishing of additively manufactured metal parts by abrasive flow machining," in *Proc. 27th Annu. Int. Solid Free. Fabr. Symp*, Austin, 2016.

[5] C. Kanger, H. Hadidi, S. Akula, C. Sandman, J. Quint, M. Alsunni and R. P. Underwood, "Effect of Process Parameters and Shot Peening on Mechanical Behavior of ABS Parts Manufactured by Fused Filament Fabrication (FFF)," in *In Solid Freeform Fabrication Symposium (SFF)*, Austin, TX, 2017.

[6] A. Q. A. Teo, L. Yan, A. Chaudhari and G. K. O'Neill, "Post-processing and surface characterization of additively manufactured stainless steel 316l lattice: Implications for biomedical use," *Materials,* vol. 14, no. 6, p. 1376, 2021.

[7] B. Rosa, P. Mognol and J.-Y. Hascoët, "Laser polishing of additive laser manufacturing surfaces," *Journal of Laser Applications ,* vol. 27, no. S2, p. S29102, 2015.

[8] C. P. Ma, Y. C. Guan and W. Zhou, "Laser polishing of additive manufactured Ti alloys," *Optics and Lasers in Engineering ,* vol. 93, pp. 171-177, 2017.

[9] Y. Tian, W. S. Gora, A. P. Cabo, L. L. Parimi, D. P. Hand, S. Tammas-Williams and P. B. Prangnell, "Material interactions in laser polishing powder bed additive manufactured Ti6Al4V components," *Additive Manufacturing,* vol. 20, pp. 11-22, 2018.

[10] G. K. Meenashisundaram, N. Wang, S. Maskomani, S. Lu, S. K. Anantharajn, S. T. Dheen, S. M. L. Nai, J. Y. H. Fuh and J. Wei, "Fabrication of Ti+ Mg composites by three-dimensional printing of porous Ti and subsequent pressureless infiltration of biodegradable Mg," *Materials Science and Engineering: C,* vol. 108, p. 110478, 2020.